

Impact of magnetic fields on polaron dynamics in low-dimensional systems

Larissa Brizhik^{a,1}, B.M.A.G. Piette^{b,2,*}

^a*Bogolyubov Institute for Theoretical Physics of the National Academy of Sciences of Ukraine, Metrologichna Str., 14-b, 03143, Kyiv, Ukraine*

^b*Department of Mathematical Sciences, Durham University, Stockton Road, DH1 3LE, Durham, United Kingdom*

Abstract

We study the impact of an external magnetic field on the long-range electron transport in quasi-one-dimensional materials, such as polypeptides, (semi)-conducting polymers and macromolecules, taking into account the electron-lattice interaction. At relatively strong electron-lattice interaction extra electrons get self-trapped in the deformation potential well and form stable bound states, called large polarons which in the continuum approximation are known as solitons. Here we do not use the continuum approximation but solve the system of discrete nonlinear equations numerically. We show that the impact of a magnetic field on polaron dynamics depends not only on the field strength, but also on the parameter values of the system which define the properties of solitons such as their energy, amplitude and width of localisation. We also study the impact of a magnetic field on a polaron created by a donor complex on a chain.

PACS numbers: 05.45.Yv, 05.60.-k, 63.20.kd, 71.38.-k

Key words: polaron, soliton, low-dimensional materials, long-range electron transport, magnetic field

*Corresponding author

¹brizhik@bitp.kyiv.ua

²b.m.a.g.piette@durham.ac.uk

1. Introduction

Recent advancements in nanotechnologies based on nanomaterials and nanostructures have stimulated the synthesis of novel low-dimensional (LD) nanomaterials with physical and chemical properties qualitatively different from those of other bulk materials. This has remarkably expanded the applications of LD compounds in numerous nanotechnologies. In particular, quasi-one-dimensional (Q1D) systems are basic units of nanorods, nanowires, and nanobelts. LD materials provide a directed path for charge carrier transport in Acceptor – Molecular Chain – Donor systems, which can occur on macroscopic distances even at room temperatures [1, 2, 3]. Among such Q1D compounds the most promising ones seem to be not only conducting polymers (CPs), but also biological macromolecules, such as polypeptides (PPs) and DNA, used in bio-nanotechnologies and biomimicring technologies.

There is a large class of such novel LD functional materials (see, e.g., [4, 5] and references therein) which enable high-performance, low-cost optoelectronic and thermoelectric devices, which are used for energy storage as well as in solar cell technologies, photonics, sensors, catalysis, coatings, etc. [6, 7, 8, 9, 10]. This raises the question of how one can explain how the highly effective conductivity of LD compounds can be stable in a broad range of physical conditions, including room and higher temperatures (see, e.g., [11]). In reply to the statement "The understanding of conduction mechanisms remains incomplete even after several decades of intensive investigation" [12], we point out that the best candidate for such a mechanism is provided by solitons, a special type of large polarons that correspond to nonlinear electron states in molecular chains, self-trapped in the deformation well due to the polaron effect [13, 14]. Such solitons in physical systems and biological macromolecules provide a long-range energy and charge transport with almost no energy dissipation. This is due to the compensation of the dispersive and nonlinear effects arising from the electron exchange interaction between neighbour sites and the electron-phonon coupling, respectively. At intermediate values of the electron-lattice coupling, solitons are extended over several lattice sites and propagate along the system as a coherent running wave. At higher concentrations, the electrons get self-trapped in a collective periodic many-soliton state similar to a charge density wave [15]. This theoretical result is supported by the fact that "There is a strong tendency for collective charge motion along the ordering direction of the polymer chains" [12, 16].

Devices based on LD materials, are often exposed to magnetic fields (MFs)

in physical conditions. Moreover, low-intensity permanent and oscillating MFs are used in non-invasive therapies. High-intensity MFs are used in diagnostic devices, such as tomography and so on. Therefore, it is important to know the impact of MFs on charge transport properties of LD materials and macromolecules. Analytically this problem has been investigated in [17] within the continuum approximation using a nonlinear perturbation method. Meanwhile it is known that the discreteness of molecular chains results in the formation of the so-called periodic Peierls-Nabarro potential relief which affects the soliton dynamics [18] and which can be critical in the presence of a MF. Therefore, here we study the impact of a MF on electron transport in LD systems using the discrete system of nonlinear equations for the electron wave function and lattice displacements, taking into account the electron-lattice interaction. For our present purposes it is not necessary to study the interaction between the self-trapped electrons, so we will use the term "polaron" as a more general term than "soliton". We consider a lattice monomer as a unit site and take into account longitudinal displacements of the sites from their equilibrium positions caused by the presence of an extra electron and electron-phonon coupling. This model is described in Section 2. The system of discrete equations does not admit exact analytical solution, so we solve them numerically. In Section 3 we discuss the known range of parameter values for CPs and macromolecules. In Section 4 we derive the equations for the Donor-Polymer system. For the numerical simulations, described in Section 5 we use 3 sets of parameters corresponding respectively to an Amide-I vibration in PPs, an extra electron in a PP and a CP. Finally, in Section 6 we summarise the obtained results, compare them with the analytical study and discuss their implications and further generalisation of the model.

2. Hamiltonian of the system and equations of motion

If we consider a one-dimensional molecular chain with an extra electron in it and take into account the electron-lattice interaction, in the absence of a magnetic field this system is described by the Fröhlich-type Hamiltonian

$$H = H_{el} + H_{latt} + H_{int}, \quad (1)$$

where the terms H_{el} , H_{latt} and H_{int} are the Hamiltonians of the electron, lattice vibrations (phonons) and electron-lattice interaction:

$$H_{el} = \sum_n \left[E_0 \Psi_n^* \Psi_n - J \left(\Psi_n^* \Psi_{n+1} + \Psi_{n+1}^* \Psi_n \right) \right], \quad (2)$$

$$H_{latt} = \frac{1}{2} \sum_n \left[M \left(\frac{dU_n}{dt} \right)^2 + \bar{W} (U_{n+1} - U_n)^2 \right], \quad (3)$$

$$H_{int} = \sum_n \bar{\sigma} \Psi_n^* \Psi_n (U_{n+1} - U_{n-1}). \quad (4)$$

Here $\Psi_n = \Psi_n(t)$ is the normalised electron wave function on the n -th site, $U_n = U_n(t)$ is the displacement of the n -th unit cell from its equilibrium position. Moreover E_0 is the on-site electron energy, M is the unit cell mass, \bar{W} is the elasticity of the bond between the nearest sites, $\bar{\sigma}$ is the electron-lattice coupling constant and J is the nearest neighbour electron exchange energy:

$$J = \frac{\hbar^2}{2ma^2} \quad (5)$$

where a is the lattice constant.

From this Hamiltonian one can derive the nonlinear system of equations for the electron wave function and lattice displacements

$$\begin{aligned} i\hbar \frac{\partial \Psi_n}{\partial t} &= E_0 \Psi_n - J (\Psi_{n+1} + \Psi_{n-1}) + \bar{\sigma} (U_{n+1} - U_{n-1}) \Psi_n, \\ M \frac{\partial^2 U_n}{\partial t^2} &= \bar{W} (U_{n+1} - 2U_n + U_{n-1}) + \bar{\sigma} (|\Psi_{n+1}|^2 - |\Psi_{n-1}|^2) \end{aligned} \quad (6)$$

which in the continuum approximation can be reduced to the nonlinear Schrödinger equation with the well-known soliton solution [13].

In the presence of a MF we have to generalise the model to a three-dimensional case and use the Peierls substitution for the electron momentum $\vec{p}(\vec{r})$ (see [17])

$$\vec{p}(\vec{r}) \rightarrow \vec{P}(\vec{r}) \equiv \vec{p}(\vec{r}) - e\vec{A} \quad (7)$$

where \vec{A} is the MF vector-potential, $\vec{B} = \text{rot}\vec{A}$, and e is the electron charge. We can represent the electron wave function as the product

$$\Psi(\vec{r}, t) = \Psi_n(t) \Psi_{tr}(y, z, t) \quad (8)$$

where $\Psi_{tr}(y, z, t)$ describes the amplitude of the electron probability distribution in the direction transverse to the chain and can be considered as depending on the continuum variables y and z . Therefore, our Hamiltonian takes the form

$$H \rightarrow H_B = H(P) + \frac{P_y^2}{2m_y} + \frac{P_z^2}{2m_z}. \quad (9)$$

Here $H(P)$ is the Hamiltonian of the chain (1) where the Peierls transformation is taken into account (7). In (9) $m_x \equiv m$, m_y and m_z are the corresponding components of the electron effective mass in the energy band.

Starting from a general gauge for the magnetic field $\vec{B} = (B_x, B_y, B_z)$ and performing the substitution $\vec{A} \rightarrow \vec{A} + \vec{\nabla}\Lambda(x, y, z)$ with the proper choice of the scalar function $\Lambda(x, y, z)$, we can pick the Landau gauge for the MF, $\vec{B} = (0, 0, B)$, with vector-potential $\vec{A} = (0, Bna, 0)$. This corresponds to the case where the MF is oriented perpendicular to the molecular chain and for which, according to the analytical study [17], the MF has the most significant impact on the polaron dynamics. For such a gauge we get from the Hamiltonian (9) the following system of equations:

$$\begin{aligned} i\hbar \frac{\partial \Psi_n}{\partial t} + J(\Psi_{n+1} + \Psi_{n-1}) - \bar{\sigma}(u_{n+1} - u_{n-1})\Psi_n &= \frac{1}{2m_y} (\hbar k_y - eBna)^2 \Psi_n, \\ M \frac{\partial^2 u_n}{\partial t^2} &= \bar{W}(u_{n+1} - 2u_n + u_{n-1}) + \bar{\sigma}(|\Psi_{n+1}|^2 - |\Psi_{n-1}|^2) \end{aligned} \quad (10)$$

where the term with E_0 (see Eq. (6)) has been excluded by a phase transformation of Ψ_n and where k_y is the y -component of the electron quasi-momentum.

To study this system, it is convenient to perform the following change of variables to use adimensional parameters:

$$\begin{aligned} \tau &= \frac{Jt}{\hbar}, \quad \xi_n = \frac{u_n}{a}, \quad \epsilon = \frac{e^2 a^2}{2m_y J}, \quad \zeta = \frac{2\pi\hbar}{ea}, \quad \zeta_0 = \frac{\hbar k_y}{ea} = \frac{\zeta}{L_y}, \\ \chi &= \frac{\bar{\sigma}a}{J}, \quad W = \frac{\hbar^2 \bar{W}}{MJ^2}, \quad \sigma = \frac{\hbar^2 \bar{\sigma}}{MJ^2 a} \end{aligned} \quad (11)$$

where L_y is the wave length corresponding to the transversal quasi-momentum k_y . Using (11), Eqs. (10) take the form

$$\begin{aligned} i \frac{\partial \Psi_n}{\partial \tau} + (\Psi_{n+1} + \Psi_{n-1}) - \chi(\xi_{n+1} - \xi_{n-1})\Psi_n &= \epsilon(nB - \zeta_0)^2 \Psi_n \\ \frac{\partial^2 \xi_n}{\partial \tau^2} &= W(\xi_{n+1} - 2\xi_n + \xi_{n-1}) + \sigma(|\Psi_{n+1}|^2 - |\Psi_{n-1}|^2). \end{aligned} \quad (12)$$

Without using perturbative methods, this system of equations does not admit exact solution. Instead, these equations can be solved numerically, but to do this we must select some specific system parameters. From a general

point of view, the system parameters not only affect the solitons properties, they actually decide on the very existence of the soliton to start with. Since we study here the impact of the MF on the electron transport on macroscopic distances, we consider large polarons, *i.e.* neither too small nor almost free electrons. Therefore, we study the obtained equations for some set of the specific numerical values close to those which correspond to realistic systems of the interest. This is discussed in the next Section.

3. Choice of system parameters

To select the system parameters we will study, we consider here two classes of systems, namely electron transport in PP macromolecules and CPs. It is estimated [13, 14, 19] that PPs have the following parameter values:

$$\begin{aligned} J &= (10^{-21} - 10^{-20}) \text{ J}, & \bar{\sigma} &= 100 \text{ pN}, & a &= 5.4 \times 10^{-10} \text{ m}, \\ \bar{W} &= (39 - 58) \text{ N/m}, & V_{ac} &= (3.6 - 4.5) \times 10^3 \text{ m/s}. \end{aligned} \quad (13)$$

It is known that the parameter values of CPs depend on physical conditions such as temperature, doping and other factors, but little is known about their numerical values, except, possibly, their sound velocity (see, e.g., [19, 20, 21] and references therein). The latter is relatively large and varies between 3000 and 9000 m/s in highly dense polymers. Summarising the available data, we can get some estimates of the other parameter values. As a model system we consider here polypyrrole and polythiophene. The former has the chemical structure $\text{H}[[\text{C}_4\text{H}_2\text{NH}]_2]_n\text{H}$ and contains two pyrrole monomers in a unit cell. Similarly, polythiophene, which has the chemical structure $\text{H}[[\text{C}_4\text{H}_2\text{S}]_2]_n\text{H}$, contains two monomers in a unit cell. In view of this we consider the following parameter values:

$$\begin{aligned} J &= (10^{-21} - 10^{-20}) \text{ J}, & \bar{\sigma} &= 100 \text{ pN}, & a &= 8 \times 10^{-10} \text{ m}, \\ M &= 216 \times 10^{-27} \text{ kg}, & V_{ac} &= (6 - 8) \times 10^3 \text{ m/s} \end{aligned} \quad (14)$$

which gives us the elasticity coefficient

$$\bar{W} = \frac{MV_{ac}^2}{a^2} = (11.25 - 20.8) \text{ N/m} \quad (15)$$

and the dimensionless electron-lattice coupling constant

$$g = \frac{\bar{\sigma}^2}{2J\bar{W}} = (0.24 - 0.77). \quad (16)$$

For this set of the parameter values the polaron is extended over several lattice sites and the amplitude of its probability in the absence of external perturbations is in the range (0.2 – 0.4).

Aside from studying the effect of MF on a perfectly formed soliton in an isolated chain, it is also appropriate to study such effect on a polaron created by a donor complex on a chain. In these cases, the polarons do not have a perfect bell-like shape but can be constituted of a few polarons, propagating at slightly different velocities. We describe this system in the next Section.

4. Donor-Polymer Systems

After analysing, in Section 5, the effect of a MF on a polaron created as a static configuration in the middle of the chain, we will also consider the effect of a MF on a polaron created by a donor complex [14]. The donor, node 0, is coupled at one end of the chain, node 1, so that, after applying the parameter scaling (11), the equations are given by

$$\begin{aligned}
i\frac{\partial\Psi_0}{\partial\tau} &= (\mathcal{E}_0 + D_d)\Psi_0 - J_d\Psi_1 + x_d\chi(\xi_1 - \xi_0)\Psi_0 + \epsilon\zeta_0^2\Psi_0, \\
i\frac{\partial\Psi_1}{\partial\tau} &= \mathcal{E}_0\Psi_1 - J_d^*\Psi_0 - \Psi_2 + \chi[x_d(\xi_1 - \xi_0) + (\xi_2 - \xi_1)]\Psi_1 + \epsilon(B - \zeta_0)^2\Psi_1, \\
i\frac{\partial\Psi_n}{\partial\tau} &= \mathcal{E}_0\Psi_n - (\Psi_{n+1} + \Psi_{n-1}) + \chi(\xi_{n+1} - \xi_{n-1})\Psi_n + \epsilon(nB - \zeta_0)^2\Psi_n, \quad n = 2, \dots, N-1, \\
i\frac{\partial\Psi_N}{\partial\tau} &= \mathcal{E}_0\Psi_N - \Psi_{N-1} + \chi(\xi_N - \xi_{N-1})\Psi_N + \epsilon(NB - \zeta_0)^2\Psi_N.
\end{aligned} \tag{17}$$

$$\begin{aligned}
\frac{\partial^2\xi_0}{\partial\tau^2} &= \frac{1}{m_d} [v_d W(\xi_1 - \xi_0) + x_d\sigma (|\Psi_0|^2 + |\Psi_1|^2)], \\
\frac{\partial^2\xi_1}{\partial\tau^2} &= v_d W(\xi_0 - \xi_1) + W(\xi_2 - \xi_1) - x_d\sigma (|\Psi_0|^2 + |\Psi_1|^2) + \sigma (|\Psi_1|^2 + |\Psi_2|^2), \\
\frac{\partial^2\xi_n}{\partial\tau^2} &= W(\xi_{n+1} - 2\xi_n + \xi_{n-1}) + \sigma (|\Psi_{n+1}|^2 - |\Psi_{n-1}|^2), \quad n = 2, \dots, N-1, \\
\frac{\partial^2\xi_N}{\partial\tau^2} &= W(\xi_{N-1} - \xi_N) - \sigma (|\Psi_N|^2 + |\Psi_{N-1}|^2),
\end{aligned} \tag{18}$$

where the index d is used to label the donor parameters and

$$J_d = \frac{\bar{J}_d}{J}, \quad x_d = \frac{\bar{\sigma}_d}{\sigma} = \frac{\chi_d}{\chi}, \quad v_d = \frac{\bar{W}_d}{W}, \quad m_d = \frac{\bar{M}_d}{M}, \quad \bar{\chi}_d = x_d\chi, \quad \mathcal{E}_0 = \frac{\bar{\mathcal{E}}_0}{J}. \tag{19}$$

In these Donor-Polymer systems, the electron is initially fully localised on the donor molecule, but as time evolves, the electron generates a few polarons travelling on the chain at slightly different velocities. This is illustrated in Figure 1 which shows the probability density of the polaron at different times, where a small polaron overtakes a larger one. The number, size and velocity of these polarons, in general, depend on the donor and the chain parameters as well as the coupling between the chain and the donor.

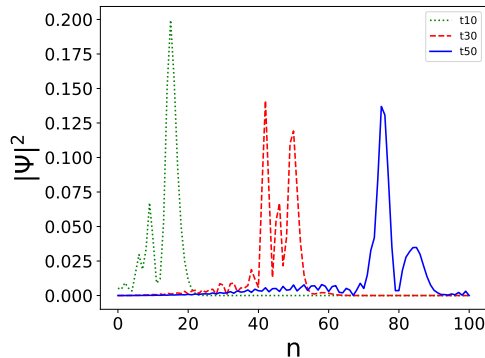


Figure 1: Time evolution of an Amide-I polaron profile on a Donor-Polypeptide system. ($\chi = 174.1$, $W = 37$, $\sigma = 0.0857$, $D_d = 0.6$, $J_d = 0.6$, $x_d = 0.2$, $v_d = 0.6$, $m_d = 5$). A small polaron overtakes a larger one.

We have performed simulations for a number of donor parameters: D_d was scanned for values in the range 0.1 to 2 by step of 0.1. J_d , X_d and V_d were all scanned for values in the range 0.1 to 1 by step of 0.1. M_d was scanned for values in the range 1 to 5 by step of 0.5. For each type of polaron, we identified the donor parameters leading to the most localised polaron reaching the end of the lattice. The values we obtained are given in table 1.

We then ran simulations with various values of the MF B and looked at the profile of the polaron when it reaches the end of the lattice chain which we chose to contain 100 nodes. We also set the transverse quasi-momentum k_y to a range of values.

x_d	x_a	D_d	J_d	$\max \Psi ^2$	N
0.1	0.1	0.6	0.7	0.183	0.75
0.3	0.3	0.6	0.7	0.201	0.81
0.6	0.6	0.8	0.7	0.219	0.82
1	1	2.2	0.9	0.251	0.89

Table 1: Optimal parameter values for the formation of a polaron on the chain with $v_d = v_a = 0.1$, $W = 0.88$, $\chi = 0.8$ and $m_d = 3$.

5. Results of numerical simulations

To solve Eqs. (12) numerically we first rewrote the equation for ξ_n as a system of pair of first order differential equations

$$\begin{aligned}
\frac{\partial \xi_n}{\partial \tau} &= \Xi_n \\
\frac{\partial \Xi_n}{\partial \tau} &= W(\xi_{n+1} - 2\xi_n + \xi_{n-1}) + \sigma(|\Psi_{n+1}|^2 - |\Psi_{n-1}|^2).
\end{aligned}
\tag{20}$$

The numerical simulations were performed by first computing the profile for the polaron by solving Eqs. (12) to which an absorbing term has been added and with $B = \zeta_0 = 0$. This was then saved as an initial profile used for further simulations, solving Eqs. (12) with non zero B and ζ_0 .

At the start of some simulations we also boosted the electron to velocity V by applying the following transformation on Ψ_n and Ξ_n

$$\begin{aligned}
\Psi_n^{(B)} &= \Psi_n \exp(iV(n - n_0)) \\
\Xi_n^{(B)} &= (\xi_{n-1} - \xi_{n+1}) \sin(V).
\end{aligned}
\tag{21}$$

For the numerical simulations, we consider three different specific systems: an Amide-I vibration polaron in a PP chain, an extra electron in a PP and an electron in a CP. The parameter values used are listed in Table 2 while the corresponding adimensional parameters are given in Table 3.

We now describe our results for the three cases considered.

5.1. Amide-I type polaron in polypeptides

The Amide-I type polaron is localised with a half width of approximately 4 lattice sites as shown in Figure 2.

Parameter	Amide-I	Extra Electron	Conducting Polymer
J (J)	1.55×10^{-22}	1.55×10^{-22}	1×10^{-21}
$\bar{\sigma}$ (N)	50×10^{-12}	50×10^{-12}	100×10^{-12}
\bar{W} (N/m)	40	40	28
M (kg)	500×10^{-27}	500×10^{-27}	500×10^{-27}
a (m)	5.4×10^{-10}	5.4×10^{-10}	5.4×10^{-10}

Table 2: Dimensional parameters for the three systems considered

Parameter	Amide-I	Extra Electron	Conducting Polymer
χ	174.19	54	80
ϵ	1.963×10^{-7}	1.963×10^{-7}	9.4542×10^{-7}
ζ (Tm)	7.6586×10^{-6}	7.6586×10^{-6}	5.1696×10^{-6}
W	37	0.62	0.628
σ	0.0857	0.0041	0.00646

Table 3: Adimensional parameters for the three systems considered. The time scale τ corresponds to 0.68ps for the Amide-I polaron and 0.1ps for the extra electron in a polypeptide or conducting polymer.

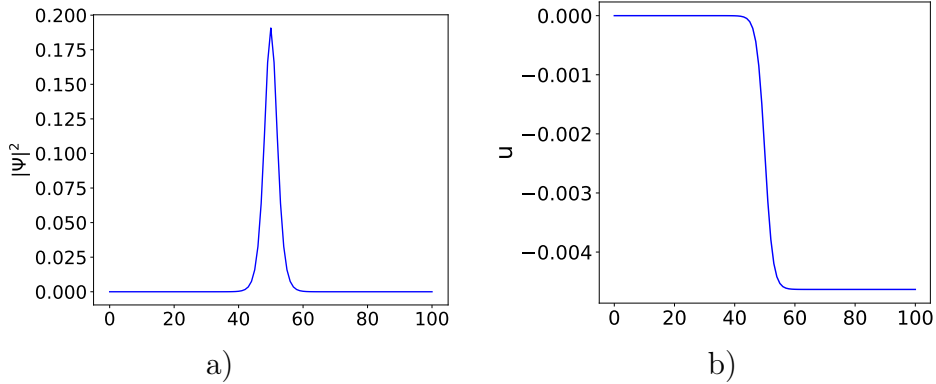


Figure 2: Amide-I type polaron ($\chi = 174.19$, $W = 37$, $\sigma = 0.0857$) as a function of n : a) profile $|\Psi|^2$; b) site displacement u .

5.1.1. The role of polaron boosts

The critical velocity, above which the polaron starts accelerating, is approximately 4.4×10^{-5} in dimensionless units. The acceleration depends on the initial boost velocity and the MF. Below the critical velocity, the polaron starts to move when $B \geq 0.2$ T. Above the critical velocity the acceleration

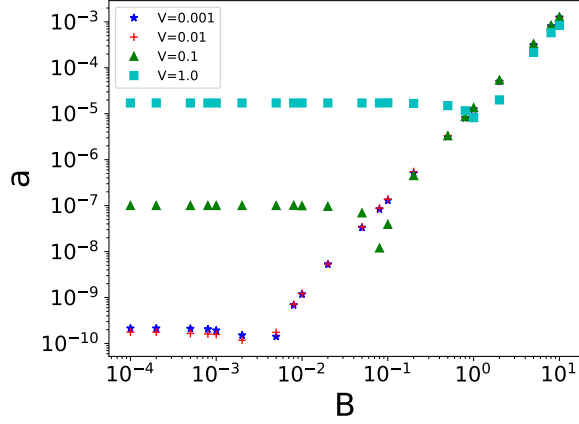


Figure 3: Amide-I type polaron: acceleration as a function of B for different boosting velocities.

varies approximately from 5×10^{-7} for $B = 0.2\text{T}$ to 1.2×10^{-3} for $B = 10\text{T}$ and to larger value when the boosting velocity is above the critical value, as shown in Figure 3.

5.1.2. Impact of the transverse quasi-momentum

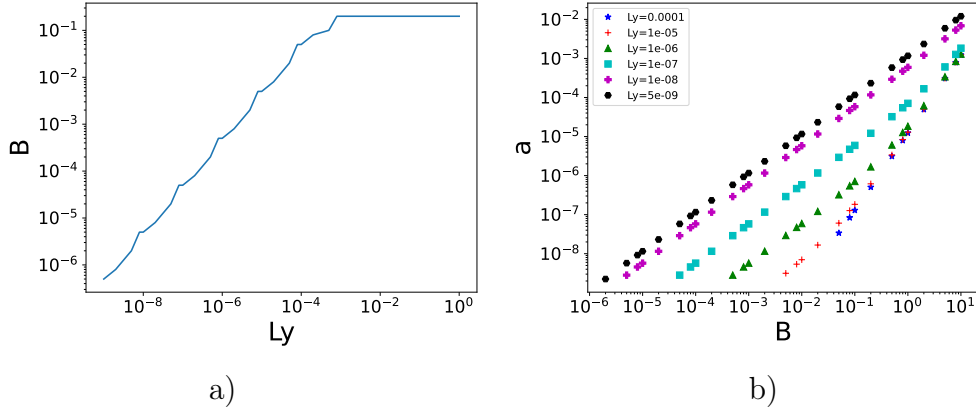


Figure 4: Amide-I polaron ($\chi = 174.19$, $W = 37$, $\sigma = 0.0857$) a) : critical B as a function of L_y ; b) acceleration as a function of B for different L_y .

At non zero transverse quasi-momentum, the critical MF required to make the polaron move depends on the transverse quasi-momentum, or correspondingly on the wavelength L_y . The critical MF is a linear function of L_y when

$L_y < 8 \times 10^{-4}\text{m}$. When $L_y \geq 8 \times 10^{-4}\text{m}$, the polaron only moves if $B \geq 0.2\text{T}$. For smaller values of L_y it starts moving for smaller values of B , as small as $B = 5 \times 10^{-7}\text{T}$ when $L_y = 10^{-9}\text{m}$. This is illustrated in Figure 4.a. The little kinks in the graph are artefacts of the sampling of B and L_y values which we have used. The acceleration depends on L_y and it is a nearly linear function of B (Figure 4.b).

5.2. Extra electron in polypeptides

The electron polaron in a PP is delocalised with a half width of approximately 5 lattice sites. The polaron profile is very similar to the one shown in Figure 2 except that the maximum of $|\Psi|^2$ is 0.17.

5.2.1. Boost

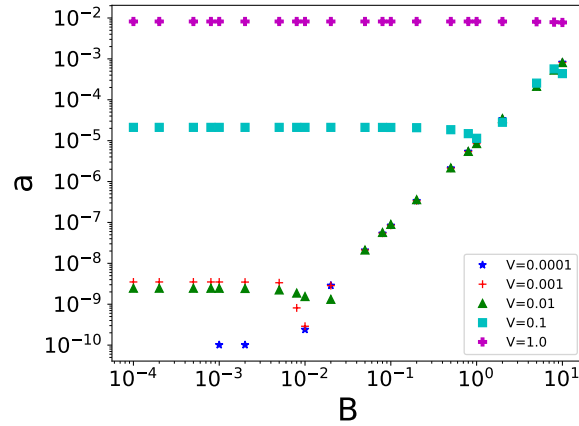


Figure 5: Extra electron in a polypeptide ($\chi = 54$, $W = 0.62$, $\sigma = 0.0041$): acceleration as a function of B for different boosts

The critical boost velocity is approximately 2.4×10^{-5} in dimensionless units. The acceleration depends on the initial boost velocity and the MF. Below the critical velocity, the polaron starts to move when $B \geq 0.05\text{T}$. Below the critical velocity the acceleration varies approximately from 2×10^{-8} for $B = 0.05\text{T}$ to 8×10^{-4} for $B = 10\text{T}$ and to larger value when the boost velocity is above the critical value, as shown in Figure 5.

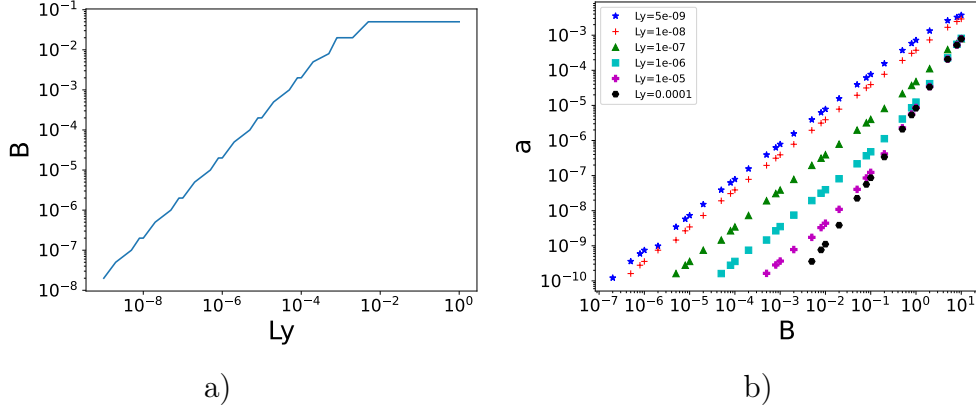


Figure 6: Extra electron in a polypeptide ($\chi = 54$, $W = 0.62$, $\sigma = 0.0041$): a) critical B ; b) acceleration as a function of B for different L_y .

5.2.2. Impact of the polaron transverse quasi-momentum

At non zero transverse quasi-momentum, the critical MF required to make the polaron move depends on the wavelength L_y corresponding to the transverse quasi-momentum. The critical MF is a linear function of L_y when $L_y < 0.002$ m. When $L_y \geq 0.002$ m, the polaron only moves if $B \geq 0.05$ T. For smaller values of L_y it starts moving for smaller values of B , as small as $B = 2 \times 10^{-8}$ T for $L_y = 10^{-9}$ m.

This is illustrated in Figure 6.a. The acceleration depends on L_y and it is a nearly linear function of B (Figure 6.b).

5.3. Conducting Polymer

The CP polaron is delocalised with a half width of approximately 3 lattice sites. The polaron profile is very similar to the one shown in Figure 2 except that the maximum of $|\Psi|^2$ is 0.34.

5.3.1. The role of polaron boosts

The critical boost velocity is approximately 0.021 in dimensionless units. As shown in Figure 7, below the critical velocity, the polaron never accelerates even when $B = 10$ T, except when the boosting velocity is slightly below the critical value ($V = 0.02$). Above the critical value, the polaron starts to accelerate when $B \leq 0.8$ T. The acceleration varies then approximately from 10^{-5} for $B = 0.8$ T to 1.5×10^{-3} for $B = 10$ T as shown in Figure 7. Surprisingly the polaron moves in the direction opposite to the boosting direction

except when the boosting velocity is slightly below the critical velocity and B is close to the minimum value to make the polaron move.

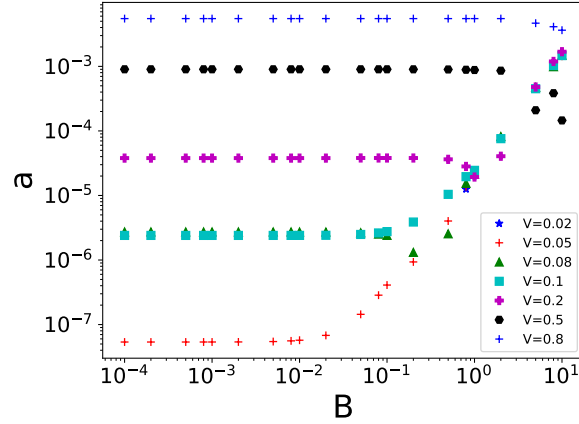


Figure 7: Conducting polymer: absolute value of the acceleration as a function of B for different boosts

5.3.2. Impact of the transverse quasi-momentum

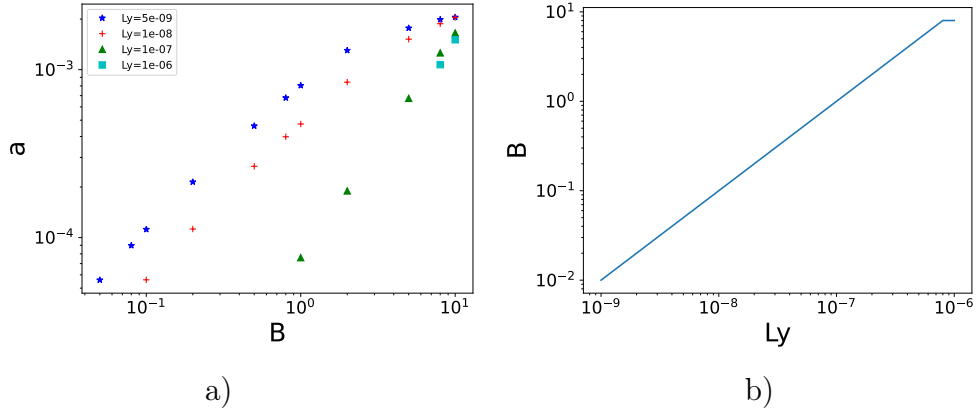


Figure 8: Conducting polymer ($\chi = 80$, $W = 0.628$, $\sigma = 0.00646$): a) acceleration as a function of B for different L_y ; b) critical B as a function of L_y

At non zero transverse quasi-momentum, the critical MF required to make the polaron move depends on the wavelength L_y and it is a linear function of L_y . When $L_y \geq 2 \times 10^{-6}$ m one needs a MF larger than 10T which we haven't

tested. When $L_y = 5 \times 10^{-9} \text{m}$, one needs a MF of at least 0.05T to move the polaron. This is illustrated in Figure 8.a. The acceleration depends on L_y and it is a nearly linear function of B (Figure 8.b).

5.4. Amide-I polaron in a Donor-Polypeptide system

For Amide-I polarons in Donor-Polypeptide systems we have chosen the following parameters:

$$\chi = 174.10, \quad \epsilon = 1.963 \times 10^{-27}, \quad \zeta = 7.6586 \times 10^{-6} \text{ mT}, \quad W = 37, \\ \sigma = 0.0857, \quad D_d = 0.6, \quad J_d = 0.6, \quad x_d = 0.2, \quad v_d = 0.6, \quad m_d = 5. \quad (22)$$

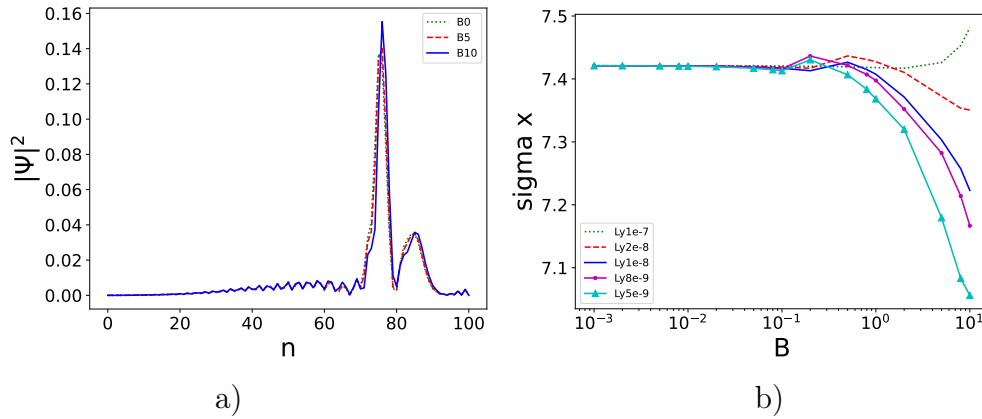


Figure 9: Amide-I polaron as a function of B ($\chi = 174.1$, $W = 37$, $\sigma = 0.0857$, $D_d = 0.6$, $J_d = 0.6$, $x_d = 0.2$, $v_d = 0.6$, $m_d = 5$): a) Polaron profile after 50 units of time; b) Width, standard deviation, of the polaron after 30.8 units of time for different values of L_y .

Figure 9.a shows several profiles of the polaron after 50 units of time when the transverse quasi-momentum is negligibly small, $L_y \gg \lambda$. We see that the effect of the MF on the polaron is negligible even when $B = 10 \text{T}$. Figure 9.b shows the average width of the polaron after reaching the middle of the lattice. We see that the polaron width does not change significantly in relatively weak MF and that for larger MF it depends on the transverse quasi-momentum.

As we can see from Figure 10, weak MFs only have a little impact on the polaron profile even when L_y is very small. This impact increases with increasing B (Figure 10). The dependence of the soliton width on the transverse quasi-momentum also increases with B . When B is large, *i.e.* well above 1T, the polaron is slightly slowed down (Figure 10.d).

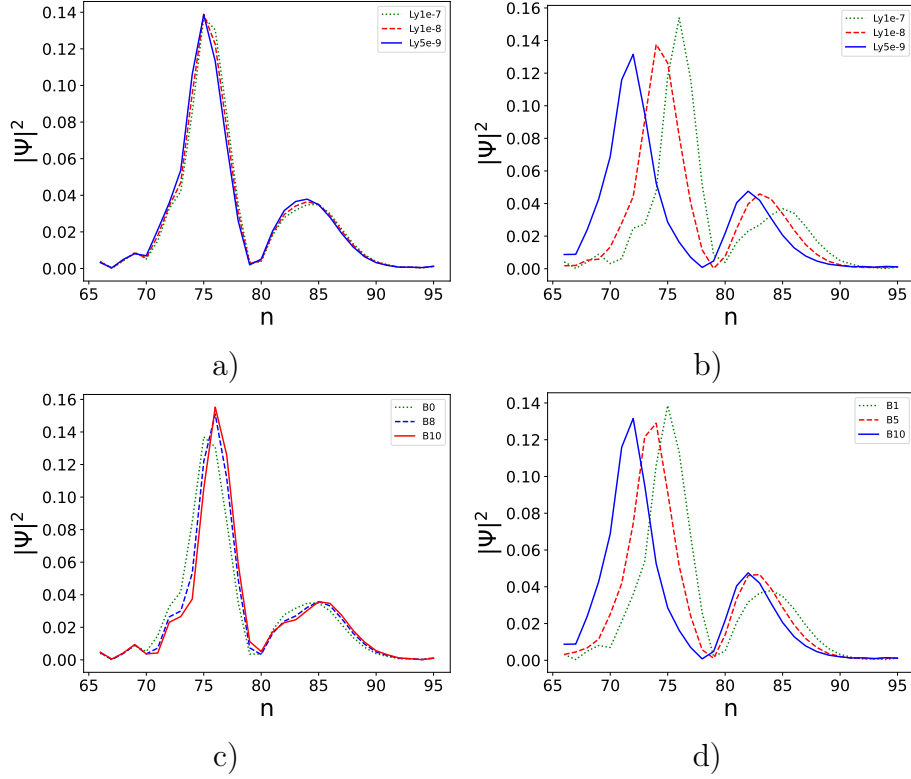


Figure 10: Profile of the Amide-I polaron in a Donor-Polypeptide system after 50 units of time as functions of B and L_y . $\chi = 174.1$, $W = 37$, $\sigma = 0.0857$, $D_d = 0.6$, $J_d = 0.6$, $x_d = 0.2$, $v_d = 0.6$, $m_d = 5$: a) $B = 1$; b) $B = 10$; c) $k_y = 0$; d) $L_y = 5 \times 10^{-9}$ (Restricted to the end of the lattice).

5.5. Electron in a Donor-Polypeptides system

For the electron polaron in a Donor-Polypeptide system we have chosen the following parameters:

$$\begin{aligned} \chi &= 54, \quad \epsilon = 1.963 \times 10^{-7}, \quad \zeta = 7.6586 \times 10^{-6} \text{ mT} \quad W = 0.62 \\ \sigma &= 0.0041, \quad D_d = 0.1, \quad J_d = 0.6, \quad x_d = 0.1, \quad v_d = 0.2, \quad m_d = 5. \end{aligned} \quad (23)$$

When the transverse quasi-momentum is very small, ($L_y \gg$), the effect of the MF is negligible (not shown) even when $B = 10\text{T}$.

Figure 11 shows the average width of the polaron profile after 27.45 units of time and we see that as B increases, the polaron becomes broader and this change of polaron width increases as the transverse quasi-momentum increases, but remains relatively small.

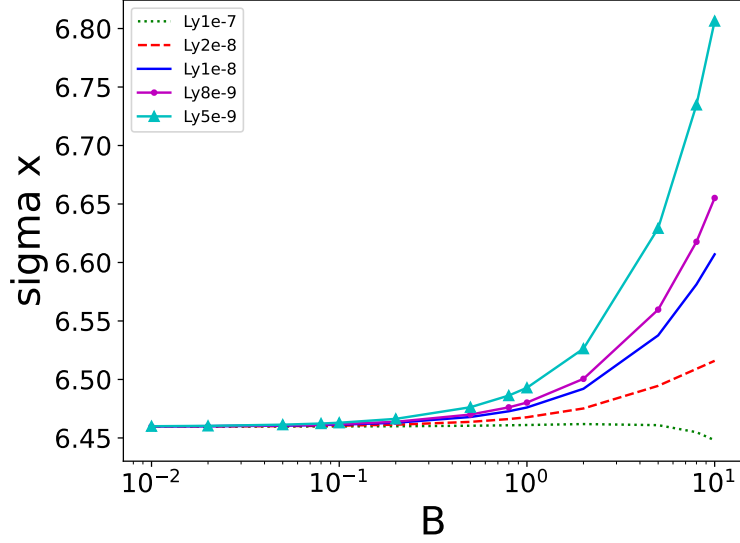


Figure 11: Width, standard deviation, of the polaron in the Donor-Polypeptide after 27.45 units of time ($\chi = 54$, $W = 0.62$, $\sigma = 0.0041$, $D_d = 0.1$, $J_d = 0.6$, $x_d = 0.1$, $v_d = 0.2$, $m_d = 5$).

As we can see from Figure 12, the MF has a very negligible effect on the polaron profile even when L_y is very small. When B is very large, *i.e.* well above 1T, the polaron is slightly slowed down (Figure 12.d).

5.6. Donor-Conducting Polymer System

$$\chi = 80, \quad \epsilon = 9.4542 \times 10^{-7}, \quad \zeta = 5.1696 \times 10^{-6} \text{ mT} \quad W = 0.628, \\ \sigma = 0.00646, \quad D_d = 0.1, \quad J_d = 0.5, \quad x_d = 0.3, \quad v_d = 0.1, \quad m_d = 5. \quad (24)$$

Figure 13.a shows several profiles of the polaron after 48 units of time when the transverse quasi-momentum is very small. We see that the effect of the MF on the polaron profile is negligible even when $B = 10\text{T}$. Figure 13.b shows that the average width of the polaron profile after reaching the middle of the lattice does not vary much as a function of B in weak MFs but increases in strong MFs. The broadening of the polaron increases as the transverse quasi-momentum becomes larger but the effect remains relatively small.

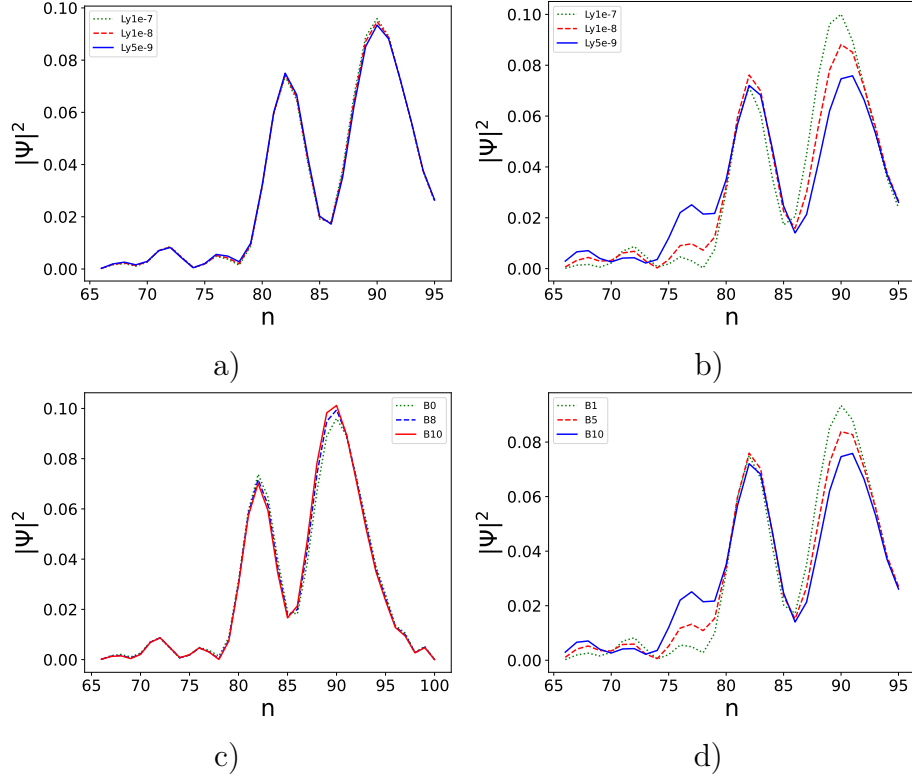


Figure 12: Profile of the polaron in a Donor-Polypeptide system after 48 units of time for several values of the magnetic field B . $\chi = 54$, $W = 0.62$, $\sigma = 0.0041$, $D_d = 0.1$, $J_d = 0.6$, $x_d = 0.1$, $v_d = 0.2$, $m_d = 5$. a) $B = 1$; b) $B = 10$; c) $k_y = 0$; d) $L_y = 5 \times 10^{-9}$.

Figure 14 shows the effect that the MF has on the polaron profile and its dependence on the transverse quasi-momentum. In the presence of a MF above the critical value, the polaron moves with a non-zero acceleration whose value depends on the MF intensity and on the transverse quasi-momentum. Despite this, the dynamics of the polaron remain stable even in strong MFs.

6. Conclusions and discussion

In this paper we have studied the numerical solutions of the coupled system of nonlinear equations that describe the dynamics of a large polaron in low-dimensional systems in the presence of an external magnetic field. We have shown that the polarons in these systems are very stable for a wide range of the parameter values while subjected to very strong magnetic fields.

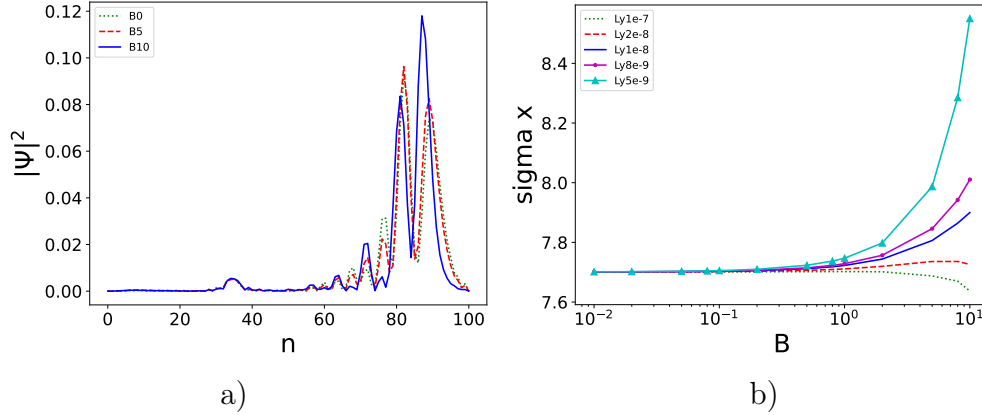


Figure 13: Polaron in a Donor-Conducting Polymer system as a function of B when $k_y = 0$ ($\chi = 80$, $W = 0.628$, $\sigma = 0.00646$, $D_d = 0.1$, $J_d = 0.5$, $x_d = 0.3$, $v_d = 0.1$, $m_d = 5$): a) Polaron profile after 48 units of time; b) Width, standard deviation, of the polaron after 28 units of time for different values of L_y .

This is true even in very long molecular chains.

The polaron dynamics is affected by the presence of a magnetic field. The characteristics of this impact depend on the field intensity, the system parameters as well as the transverse quasi-momentum of the polaron. Unlike for the analytical solution described in [17], in a discrete system there is some critical value of the magnetic field and the polaron transverse quasi-momentum above which the polaron can start moving when it's initial velocity is zero. We have also studied the dynamics of the polaron after it was boosted and showed that in relatively strong magnetic fields the polaron is accelerated confirming the results of our previous analytical study [17].

Our study shows that when the polaron is broader, one requires a larger boost velocity to make the polaron move. This can be explained by the fact that as a broader polaron spans over more lattice sites, the lattice phonons of the polaron have a larger kinetic energy.

These results were obtained for a large range of system parameters, characteristic of the Amide-I-type polaron and electron polarons in polypeptide macromolecules, as well as for electrons in conducting polymers, like polypyrrole and polythiophene. We have considered magnetic fields up to 10 T as the most typical magnetic fields existing in laboratory or used in various appliances.

We have also studied the impact of magnetic fields on the dynamics of

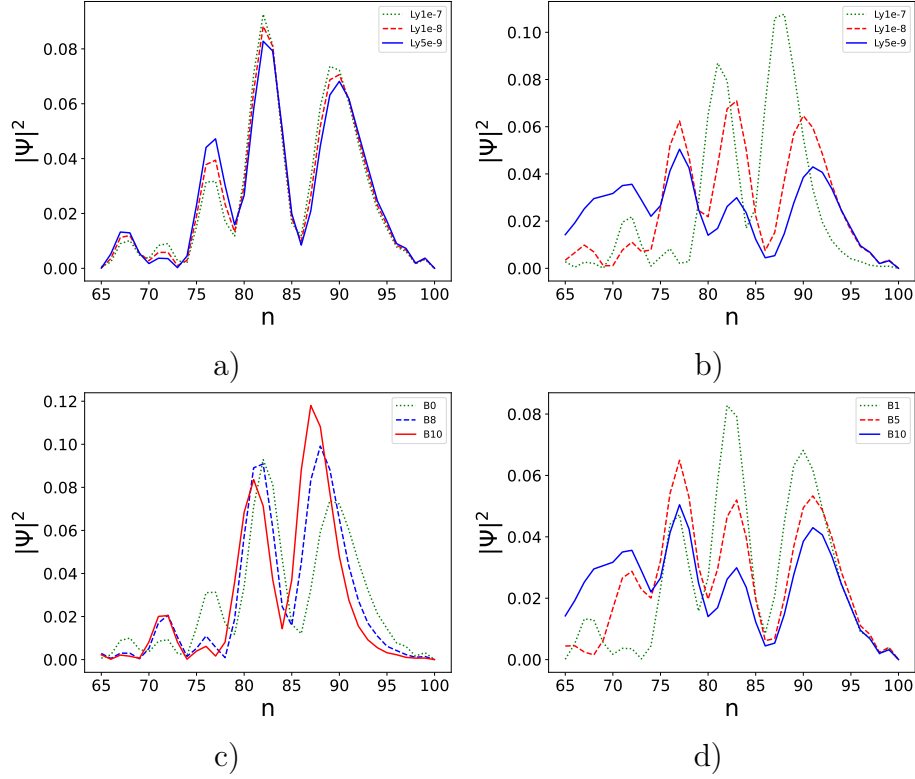


Figure 14: Polaron profile in a Donor-Conducting system after 48 unit of time for several values of the magnetic field. $\chi = 80$, $W = 0.628$, $\sigma = 0.00646$, $D_d = 0.1$, $J_d = 0.5$, $x_d = 0.3$, $v_d = 0.1$, $m_d = 5$. a) $B = 1$; b) $B = 10$; c) $k_y = 0$; d) $L_y = 5 \times 10^{-9}$.

polarons in Donor-Molecular Chain complexes where an electron, initially fully localised at the donor, tunnels to the chain and generates, after a finite time, a polaron on the chain. We have also shown that the localised electron generated by such Donor complex, for the studied parameter values, is made of a few polarons travelling at slightly different velocities but leading to a highly efficient electron transport in very long chains of up to 100 monomer units. This transport was only slightly affected even by the stronger magnetic fields, allowing us to conclude that large soliton-like polarons provide a highly effective long-range electron transport even in the presence of strong external magnetic fields.

7. Acknowledgements

LB acknowledges grant 2025.07/0335 of the Fundamental Research Foundation of Ukraine and the support of the INI-LMS Rebuild Ukraine Scheme at the Department of Mathematical Sciences of the University of Durham (UK).

References

- [1] Nicole L. Ing, Mohamed Y. El-Naggar, and Allon I. Hochbaum. Going the distance: Long-range conductivity in protein and peptide bioelectronic materials. *The Journal of Physical Chemistry B*, 122(46):10403–10423, Nov 2018.
- [2] Nadav Amdursky. Enhanced solid-state electron transport via tryptophan containing peptide networks. *Phys. Chem. Chem. Phys.*, 15:13479–13482, 2013.
- [3] Yan Zhu, Richard Champion, and Samson Jenekhe. Conjugated donor-acceptor copolymer semiconductors with large intramolecular charge transfer: Synthesis, optical properties, electrochemistry, and field effect carrier mobility of thienopyrazine-based copolymers. *Macromolecules*, 39, 11 2006.
- [4] Si Young Ban, Xuchen Nie, Zhihao Lei, Jiabao Yi, Ajayan Vinu, Yang Bao, and Yanpeng Liu. Emerging low-dimensional materials for nano-electromechanical systems resonators. *Materials Research Letters*, 11:21 – 52, 2022.
- [5] Chamikara Karunasena, Jonathan Thurston, Thomas Chaney, Hong Li, Chad Risko, Veaceslav Coropceanu, Michael Toney, and Jean-Luc Bredas. Polymorphs of the n-type polymer p(ndi2od-t2): A comprehensive description of the impact of processing on crystalline morphology and charge transport. *Advanced Functional Materials*, 35, 01 2025.
- [6] Tao Jia, Jiabin Zhang, Wenkai Zhong, Yuanying Liang, Kai Zhang, Sheng Dong, Lei Ying, Feng Liu, Xiaohui Wang, Fei Huang, and Yong Cao. *Nano Energy*, 72:104718, 2020.

- [7] Dhiman Bhattacharyya, Rachel M. Howden, David C. Borrelli, and Karen K. Gleason. Vapor phase oxidative synthesis of conjugated polymers and applications. *Journal of Polymer Science Part B: Polymer Physics*, 50(19):1329–1351, 2012.
- [8] Bed Poudel, Qing Hao, Yi Ma, Yucheng Lan, Austin Minnich, Bo Yu, Xiao Yan, Dezhi Wang, Andrew Muto, Daryoosh Vashaee, Xiaoyuan Chen, Junming Liu, Mildred S. Dresselhaus, Gang Chen, and Zhifeng Ren. High-thermoelectric performance of nanostructured bismuth antimony telluride bulk alloys. *Science*, 320(5876):634–638, 2008.
- [9] T. Huang, X. Huang, C. Hu, J. Wang, H. Liu, Z. Ma, J. Zou, and W. Ding. Enhancing hydrogen storage properties of mgh₂ through addition of ni/comoo₄ nanorods. *Materials Today Energy*, 19:100613, 2021.
- [10] Wanru Xu, Yilin Chang, Xiangwei Zhu, Zhenhua Wei, Xiaoli Zhang, Xiangnan Sun, Kun Lu, and Zhixiang Wei. Organic solar cells based on small molecule donor and polymer acceptor. *Chinese Chemical Letters*, 33(1):123–132, 2022.
- [11] Rama Venkatasubramanian, Edward Siivola, Thomas Colpitts, and Brooks O’Quinn. Thin-film thermoelectric devices with high room-temperature figures of merit. *Nature*, 413(6856):597–602, Oct 2001.
- [12] Asli Ugur, Ferhat Katmis, Mingda Li, Lijun Wu, Yimei Zhu, Kripa K. Varanasi, and Karen K. Gleason. Low-dimensional conduction mechanisms in highly conductive and transparent conjugated polymers. *Advanced Materials*, 27(31):4604–4610, 2015.
- [13] A. S. Davyov. *Solitons in Molecular Systems*. Reidel, Dordrecht, 1991.
- [14] L. S. Brizhik, B. M. A. G. Piette, and W. J. Zakrzewski. Donor-acceptor electron transport mediated by solitons. *Phys. Rev. E*, 90:052915, Nov 2014.
- [15] Larissa Brizhik. *Electron Correlations in Molecular Chains*, pages 215–232. 04 2017.
- [16] H. Sirringhaus, P. J. Brown, R. H. Friend, M. M. Nielsen, K. Bechgaard, B. M. W. Langeveld-Voss, A. J. H. Spiering, R. A. J. Janssen, E. W. Meijer, P. Herwig, and D. M. de Leeuw. Two-dimensional charge

- transport in self-organized, high-mobility conjugated polymers. *Nature*, 401(6754):685–688, October 1999.
- [17] Larissa Brizhik. Dynamics of the Davydov’s soliton in external oscillating magnetic field. *Chaos Solitons and Fractals*, 187:115459, October 2024.
- [18] Larissa Brizhik, Alexander Eremko, Leonor Cruzeiro-Hansson, and Yulia Olkhovska. Soliton dynamics and peierls-nabarro barrier in a discrete molecular chain. *Phys. Rev. B*, 61:1129–1141, Jan 2000.
- [19] M. Gulácsi, M.A.M. El-Mansy, and Z. Gulácsi. Electron-phonon interactions in conducting polymers. *Philosophical Magazine Letters*, 96(2):67–75, 2016.
- [20] Thanh-Hai Le, Yukyung Kim, and Hyeonseok Yoon. Electrical and electrochemical properties of conducting polymers. *Polymers*, 9(4), 2017.
- [21] Ilaria Abdel Aziz, Gabriele Tullii, Maria Rosa Antognazza, and Miryam Criado-Gonzalez. Poly(3-hexylthiophene) as a versatile semiconducting polymer for cutting-edge bioelectronics. *Mater. Horiz.*, 12:5570–5593, 2025.